Avrupa Bilim ve Teknoloji Dergisi
Sayı 23, S. 456-464, Nisan 2021

Araştırma Makalesi

www.ejosat.com ISSN:2148-2683

European Journal of Science and Technology
No. 23, pp. 456-464, April 2021

Research Article

Forecasting The Biosorption of Crystal Violet Cationic Dye onto Biomass-driven Graphene-Like Porous Carbon Through Artificial Neural Network Approach

Ceren Karaman[1*]

[1*] Akdeniz University, Vocational School of Technical Sciences, Departmant of Electricity and Energy, Antalya, Turkey, (ORCID: 0000-0001-9148-7253), cerenkaraman@akdeniz.edut.tr

(First received 11 February 2021 and in final form 4 April 2021)

(**DOI:** 10.31590/ejosat.878772)

ATIF/REFERENCE: Karaman, C. (2021). Forecasting The Biosorption of Crystal Violet Cationic Dye onto Biomass-driven Graphene-Like Porous Carbon Through Artificial Neural Network Approach. *European Journal of Science and Technology*, (23), 456-464.

Abstract

Textile industries are considered to be the main actors in water pollution. Estimation of the textile dye sorption capacities of the biosorbents/adsorbents are crucial as design considerations. Herein, the feasibility of utilizing orange-peel-derived graphene-like porous carbons (GCs) as a low-cost biosorbent for removal of Crystal Violet (CV) cationic dye from aqueous solution have been evaluated both by batch biosorption experimental-setup and by using an artificial neural network (ANN) approach. The physicochemical characterization results have indicated that as-synthesized GCs has a specific surface area of 985 $m^2.g^{-1}$, a pore volume of 1.04 $cm^3.g^{-1}$, and a point of zero charge (pH_{PZC}) of 6.50. The biosorption capacity of the biosorbent has been investigated as a function of initial pH, bisorbent dosage, initial dye concentration, and temperature. The optimal biosorption performance values have been achieved at pH of 7.5, the biosorbent dosage of 3.0 $g.L^{-1}$, the temperature of 25 ℃, in which 91.6% of initial CV (initial dye concentration of 100 ppm) has been successfully removed. The experimental results have indicated that the biosorption process significantly depends on the temperature whereas *ca.*15 min of contact time is sufficient for reaching equilibrium. The ANN approach has been utilized to forecast the biosorption performance of GCsThe proposed ANN model has been trained by the Levengberg-Marquardt backpropagation algorithm, by using the activation function of purelin and tansig functions at hidden and output layers, respectively. Different hidden topologies have been evaluated to optimize the ANN model. An optimal ANN model structured with two hidden layers with 5 and 10 neurons in each layer has been developed to forecast the biosorption of CV with high-performance parameters (linear correlation coefficient, *R*= 0.9995; mean squared error, *MSE*=0.0004). This work has shown that the experimental data are in harmony with ANN-based data, so it can be speculated that the proposed ANN approach can be utilized for predicting the cationic dye biosorption

Keywords: Agricultural Waste, Artificial Neural Network (ANN), Biosorption, Crystal Violet, Modeling, Orange Peel.

Yapay Sinir Ağı Yaklaşımı ile Crystal Violet Katyonik Boyarmaddesinin Biyokütle-temelli Grafen Benzeri Gözenekli Karbon Üzerine Biyosorpsiyonunun Tahmin Edilmesi

Öz

Tekstil endüstrisi su kirliliğinde ana aktörler olarak kabul edilmektedir. Biyosorbentlerin / adsorbanların tekstil boyası soğurma kapasitelerinin tahmini, tasarım konuları olarak çok önemlidir. Bu çalışmada, sulu çözeltiden Crystal Violet (CV) katyonik boyarmaddesinin uzaklaştırılması için düşük maliyetli bir biyosorbent olarak portakal kabuğu türevi grafen benzeri gözenekli

[*] Corresponding Author: cerenkaraman@akdeniz.edu.tr

karbonun (GCs) kullanılmasının fizibilitesi hem kesikli biyosorpsiyon deney düzeneği ile hem de yapay bir sinir ağı (YSA) yaklaşımı kullanılarak değerlendirilmiştir. Fizikokimyasal karakterizasyon sonuçları, sentezlenen GCs'nin 985 $m^2.g^{-1}$ özgül yüzey alanına, 1.04 $cm^3.g^{-1}$ gözenek hacmine ve 6.50 sıfır yük noktasına (pH_{PZC}) sahip olduğunu ortaya çıkarmıştır. Biyosorbentin biyosorpsiyon kapasitesi, başlangıç pH'ı, bisorbent dozu, başlangıç boya konsantrasyonu ve sıcaklığın fonksiyonu olarak araştırılmıştır. En yüksek biyosorpsiyon performans değerleri pH 7.5, biyosorbent konsantrasyonu 1.0 $g.L^{-1}$, 25 ° C sıcaklıkta elde edilmiştir ve burada başlangıçtaki CV'nin% 91.6 'si başarıyla uzaklaştırılmıştır. Deneysel sonuçlar, biyosorpsiyon işleminin önemli ölçüde sıcaklığa bağlı olduğunu, ancak yaklaşık 15 dakikalık temas süresinin dengeye ulaşmak için yeterli olduğunu göstermiştir. GC'nin biyosorpsiyon performansını tahmin etmek için YSA yaklaşımı kullanılmıştır. Önerilen YSA modeli, sırasıyla gizli katmanda ve çıktı katmanlarında purelin ve tansig fonksiyonlarının aktivasyon fonksiyonu kullanılarak, Levengberg-Marquardt geri yayılım algoritması ile eğitilmiştir. YSA modelini optimize etmek için farklı gizli topolojiler değerlendirilmiştir. Yüksek performanslı parametrelerle (doğrusal korelasyon katsayısı, R = 0.9995; ortalama kare hatası, MSE = 0.0004) CV'nin biyosorpsiyonunu tahmin etmek için 5 ve 10 nöronlu iki gizli katman ile yapılandırılmış optimal bir YSA modeli geliştirilmiştir. Bu çalışma, deneysel verilerin YSA temelli verilerle uyumlu olduğunu ortaya koymuştur, bu nedenle önerilen YSA yaklaşımının katyonik boyarmadde biyosorpsiyonunu tahmin etmek için kullanılabileceği söylenebilir.

Anahtar Kelimeler: Tarımsal Atık, Yapay Sinir Ağı (YSA), Biyosorpsiyon, Crystal Violet, Modelleme, Portakal Kabuğu.

1. Introduction

The exponential increase in industrialization especially in textile, leather, paper, printing, food, cosmetic, petroleum industries has led to severe contamination of groundwater due to their synthetic dye pollutants. Almost 15% of dyes are wasted during the process and *ca.*20% of them have been directly discharged to wastewater. Hence, they threaten both many of the life forms and the environment. There are almost theree hundered types of dyes readily available. Amongst them, synthetic dyes are the main threat due to their non-biodegradable, highly stable and toxic nature (Karaman and Aksu, 2020). Crystal violet, one of the well-known cationic synthetic dye, is utilized in various applications such as cosmetics, veterinary medicine, textile dyeing, printing, dermatology, an additive to poultry feed. Even a trace amount of it may cause cytotoxic and carcinogenic effects on cells and severe damage to the cornea and conjunctiva, besides the adverse effects on the aquatic life. Therefore, so far number of researches have been conducted for the removal of organic pollutants to protect both human beings and the environment. In addition to conventional technologies for water treatment, the researchers have intensely focused on alternative techniques such as membrane process, electrosorption, photocatalytic oxidation, and of course adsorption which is one of the most promising candidates (Kodal and Aksu, 2017). Adsorption is considered to be one of the most feasible ones since it offers high removal efficiency, low-cost and operation simplicity, suitable for scaling-up (Karaman and Aksu, 2020; Karaman 2020). Among the variety of biomaterials that can be used as biosorbents, agricultural wastes have gained substantial prominence due to their low-cost, availability, non-toxicity, environmental benignity, and the possibility to obtain various derivatives. Among the various types of agricultural waste biosorbents, orange peel is considered to be a satisfactory biosorbent since its surface functionality and lignocellulosic structure, as well as its readily available (Karaman 2020; Liang et al., 2009; Lu et al., 2009; Pathak et al., 2016).

In the adsorption/biosorption process there are many interactions between the adsorbent/biosorbent and the adsorbates that mainly influenced by operational conditions. Especially in large-scale applications, it is vital to utilize a smart model to forecast the removal efficiency of biosorbents without conducting redundant efforts. In this sense, the ANN approach that is one of the powerful candidates to model both linear and non-linear systems can be successfully applied to modeling the adsorption process, and also optimize the process (Dehghani et al., 2020; Pauletto et al., 2020). It is noteworthy that the performance of the ANN model depends on its structure such as selected backpropagation algorithm, activation function in hidden/output layers, and the number of neurons and hidden layers (Pauletto et al., 2020; Elemen et al., 2012, Fawzy et al., 2018; Ghaedi et al., 2014). Thus, it is important to optimize the proposed ANN model (Pauletto et al., 2020). There are several valuable works that get benefits from ANN to predict the adsorption behavior of the various systems. Broujeni et al. (2021) synthesized chitosan/TiO_2 nanocomposite and investigated its application as an adsorbent for removing thorium (IV) (Th^{4+}) ion from aqueous solution. All experiments were carried out by ANN, and genetic algortihm was implemented to determine the most suitable operating condition for the adsorption of Th^{4+}. Hanandeh et al. (2021) simulated Pb, Cu and Ni adsorption in single and multicomponent solutions by constructed different machine learning algorithms specifically ANN models. They reported that the Bayesian regularization backpropogation algorithm offered the highest accuracy amongst the others. Additionally, it was stated that the best performance was achieved by using 8 neurons in the hidden layer with symmetrical logistic transfer functions (tansig) for both the hidden and output layers. Based on the above facts, it can be speculated that related studies on biosorbent can also be applied to other optimized ANN models. Herein, a cost-natural orange-peel-derived graphene-like porous carbon has been utilized as biosorbent for removal of cationic dye from aqueous solutions. It is aimed to get further insight in the biosorption of crystal violet dye onto GCs both by conducting batch biosorption experiments and by applying the proposed ANN model to validate and forecast the removal efficiency. Even though there are plenty of reported works on the orange peel derived bisorbents for dye removal, this work is original as it highlights the biosorption of CV onto GCs by ANN approach. The maximum dye removal efficiency of the GCs and optimum process conditions have been determined by assesing the independent variables including initial pH of the solution, initial dye concentration ($mg.L^{-1}$), biosorbent dosage ($g.L^{-1}$), and operation temperature (℃). These independent variables have been used as input data for the proposed ANN model, whereas the removal efficiency is the output data. The ANN model has been optimized by evaluating the different hidden layer topologies. The ANN model has been trained by the Levengberg-Marquardt backpropagation algorithm, by using the activation function of purelin and tansig functions at hidden and output layers, respectively. The ANN

performance has been evaluated by well-established performance metrics including mean squared error and linear determination coefficient to forecast the CV removal efficiency of the GCs by using the testing data.

2. Methodology

2.1. Synthesis of Biosorbent

The waste orange peel-derived graphene-like porous carbon biosorbents were synthesized according to our previous report (Karaman, 2020). The schematic representation of the proposed two-step production pathway was given in Scheme 1. The washed, ball-milled, and dried waste orange peels (DOP) were used as a carbon precursor to synthesize GCs. A two-step facile route consisting of thermal annealing and the chemical activation with potassium hydroxide (KOH) was applied for preparing GCs biosorbents. As-prepared powder was treated with 0.1 M hydrochloric acid (HCl) and deionoized water (DI) to remove inorganic salts. Afterward, the product was dried at 70 °C in a vacuum oven, then labeled as GCs.

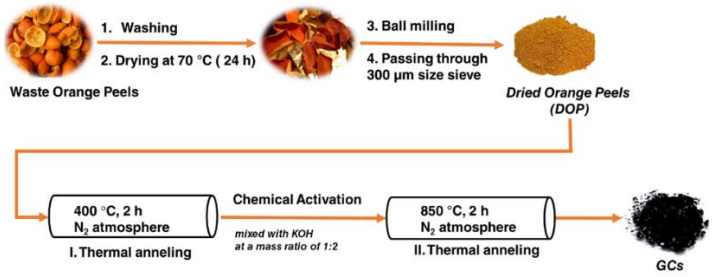

Scheme 1. Schematic illustration of synthesis pathway for GCs

2.2. Preparation of Crystal Violet Solution

Crystal violet solutions with determined initial CV concentrations (listed in Table 1) was prepared by from 1000 ppm stock solution of CV. Subsequently, the initial pH (range between 2.0-10.0) of dye solutions were set by using 0.1 N HCl and 0.1 N NaOH solution, followed by the biosorbent was added to the pH-adjusted dye solution.

2.3. Physicochemical Characterization of Biosorbent

The physicochemical characterization of GCs was conducted by field-emission scanning electron microscope (FE-SEM) (Hitachi S-4900) operating at 5.0 kV, and transmission electron microscope (TEM, JEM-1400F, JEOL) at 120 kV. The Brunauer–Emmett–Teller surface areas (S_{BET}) of biosorbent were obtained with the help of the N_2 adsorption/desorption measurements (at 77 K) by using Quantachrome Nova 2200 automated surface area analyzer (Quantachrome Corporation, USA). The pore size distributions (PSD) were calculated by the Barrett-Joyner-Halenda (BJH) method.

2.4. Experimental Studies of Batch Biosorption

Series of typical batch biosorption experiments were conducted as reported in the previous report (Karaman, 2020) to investigate the effect of independent variables (Table 1) on CV removal efficiency. During the experimental studies, t_0 was defined as the time when a weighed amount of GCs was first introduced to 100 mL of pH-adjusted test solution. Subsequently, at pre-determined contact time intervals up to 120 min, periodically 5.0 mL of dye samples were taken out, followed by centrifugation at 5000 rpm for 5 min. The residual CV concentration was determined by a UV/Vis spectrophotometer (U–2800, Hitachi, Japan) at the maximum adsorption peak (λ_{opt}).

Table 1. Range of biosorbtion operating condition variables

Independent variables	Range
Initial pH of the dye solution	2.0, 3.5, 4.0, 5.5, 6.0, 7.5, 8.5, 10.0
Initial CV concentration (ppm)	25.0, 50.0, 100.0, 250.0, 500.0, 750.0
Dosage of GCs (g.L^{-1})	1.0, 1.5, 2.0, 3.0, 4.0 5.0
Operation temperature (°C)	25, 35, 45

2.4.1. Evalutaion of Biosorption Performance

The biosorption capacity q (mg. g^{-1}) (Eq. 1), removal efficiency % (Eq. 2), and biosorption rate r (mg.g^{-1}.min^{-1}) (Eq.3) metrics of the GCs were calculated.

$$q = \frac{(C_0 - C)}{X} \quad (1)$$

$$\text{removal efficiency } \% = \frac{(C_0 - C)}{C_0} \times 100 \quad (2)$$

$$\text{r} = \frac{\Delta q}{\Delta t} \quad (3)$$

where C_o (mg.L^{-1}) is the initial arsenate concentration; C (mg.L^{-1}) is the residual arsenate concentration at any time of the biosorption process; X is the biosorbent dosage (g.L^{-1}); t is the time (min).

The experiments were performed in triplicate to guarantee the accuracy and the reproducibility of the data, and the average of them was used in data processing conducted by Microsoft Excel 2010. The relative standard deviations were calculated to be within ±3 %.

2.4. Artificial Neural Network Modeling

The neural network toolbox of MatLab® 9.5 (R2018b) software was utilized to train and simulate the ANN network for forecasting the CV removal efficiency of as-synthesized GCs. The proposed feedforward ANN model consisting of interconnected input, hidden and output layers was trained by the Levenberg-Marquardt (*trainlm*) backpropagation algorithm, using the activation function of purelin (Eq. 4) and tansig (Eq.5) at the hidden and the output layers, respectively.

$$y = purelin(x) = x \quad (4)$$

$$y = tansig(x) = \frac{2}{(1+\exp(-2x))-1} \quad (5)$$

The experimental data were randomly divided into training data (70%), validation data (15%), and test data (15%). The data were previously normalized to the range of -1 to 1 by MatLab® function *mapminmax* to avoid the overfitting problem and maintain the generalization. The initial pH of the solution, initial dye concentration, biosorbent dosage, and the operating

temperature were the input neurons of the proposed model, whereas the removal efficiency was the neuron of the output layer. The number of artificial neurons in hidden layers is mainly responsible for feature extraction from the input to predict the output. Thus, the performance of the developed ANN model depends on the number of hidden layers and the number of artificial neurons in these layers. Therefore, different hidden layer topologies based on degrees of freedom analysis of the system were evaluated to optimize the ANN model.

The performance of the proposed model and the optimal hidden topology were chosen based on the performance metrics of MSE (Eq. 6) and R (Eq. 7) values.

$$MSE = \frac{1}{N}\sum_{i=1}^{N}\left(\left|y_{prd,i} - y_{exp,i}\right|\right)^2 \quad (6)$$

$$R = 1 - \frac{\sum_{i=1}^{N}(y_{prd,i} - y_{exp,i})}{\sum_{i=1}^{N}(y_{prd,i} - y_M)} \quad (7)$$

where $y_{prd,i}$ is the predicted value by ANN model, $y_{exp,i}$ is the experimental value, y_M is the average of experimental value, and N is the number of data.

3. Results and Discussion

3.1. Physicochemical Characterization of Biosorbent

SEM and TEM analysis were conducted to investigate the morphology and the structure of as-synthesized samples (Figure 1). The SEM migrograph of DOP (Figure 1a) suggested irregular-shaped bulk carbon monoliths. On the otherhand, the SEM images of GCs sample presented silky porous network with micro and mesoporous structure (Figure 1b). As presented in Figure 1c, TEM image of GCs sample offered slightly wrinkled surface characteristics of graphene structures besides atomic-thick layered carbon material.

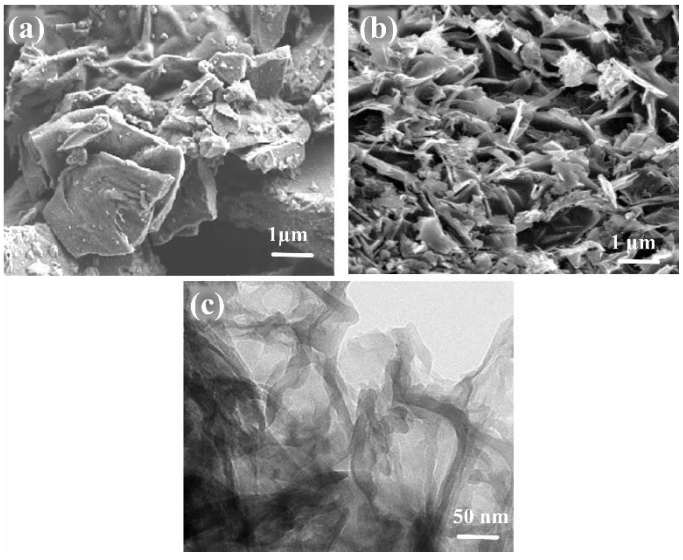

Figure 1. FE-SEM images of (a) DOP and (b) GCs, (c)TEM image of GCs

The BET surface areas (Figure 2a) and the PSDs (Figure 2b) of as-sythesized samples were calculated and tabulated in Table 2. The increment in the S_{BET} value of GCs mainly attributed to the activation of the mesopores and micropores of samples by KOH activation and thermal annealing. The observed Type-IV hysteresis loop in N_2 adsorption/desorption isotherm of GCs suggested dominant mesoporous structures which also was confirmed by the PSD analysis. As listed in Table 2, thanks to the higher S_{BET} and hierarchically-ordered micro and mesoporous structure with large pore volume of GCs, the dye adsorption capacity of GCs was expected to be higher than DOP.

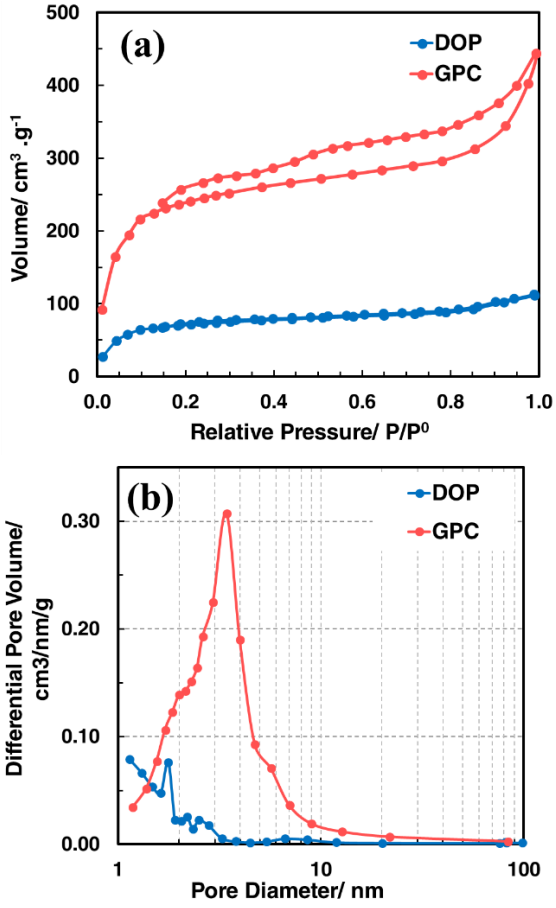

Figure 2. (a) N_2 adsorption/desorption isotherms (b) the BJH pore size distributions of DOP and GCs

Table 2. Physicochemical parameters obtained from N_2 adsorption/desorption isotherms of DOP and GCs samples

Sample ID	S_{BET} $m^2.g^{-1}$	V_{micro} $cm^3.g^{-1}$	V_{meso} $cm^3.g^{-1}$	V_{total} $cm^3.g^{-1}$	V_{micro} %	V_{meso} %
DOP	102.0	0.10	0.05	0.14	67.38	32.62
GCs	985.0	0.41	0.63	1.04	39.85	60.15

3.2. Effect of Experimental Parameters on CV Removal

3.2.1. Initial pH

The effect of solution initial pH on the biosorption of CV, a serial of batch biosorption studies were carried out over a pH range of 2.0-10.0 at 100 ppm initial CV concentration, and 1.0 $g.L^{-1}$ GCs dosage. The results indicated that the pH of the solution directly affect the biosorption capacities of the biosorbent (Figure 3). The dye removal efficiency of increased at the alkaline media up to pH 7.5. It has been observed that there was no remarkable change in removal efficiency. Therefore, further experiments were conducted at pH 7.5. However, it should be noted that the slight decrease in the removal efficiency at alkaline media was mainly caused by the competition of hydroxyl ions and the crystal violet oxyanions

(Abid et al., 2016; Rahaman et al., 2008). It is noteworthy to emphasize that the neutral pH values give the way for practical application for textile wastewater treatment. The results were consistenwith the zeta potential measurements. The point of zero charge (pH_{PZC}) of GCs was measured as 6.50. At a higher pH value than pH_{PZC} of the sample, the surface of the biosorbent charged negatively and led to favor the biosorption of cationic species. On the other hand, the lower pH_{PZC} values, the surface protonated and prone to biosorp the anionic species (Das et al., 2007; Su et al., 2010). In the light of these findings, it could be proposed the biosorption of CV onto GCs probably occurred as a result of electrostatic interaction.

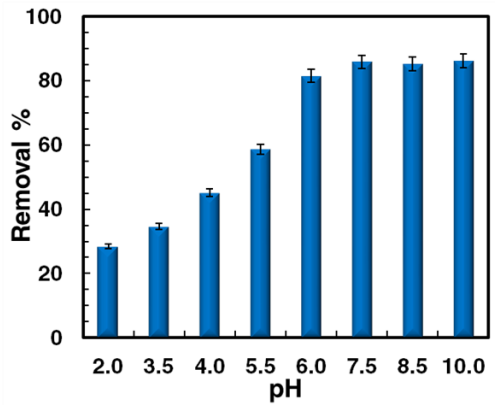

Figure 3. Effect of the initial pH of the dye solution on the removal efficiency of GCs (C_o=100 ppm, X=1.0 g.L^{-1}; t=120 min, T= 25 ℃).

3.2.2. GCs Dosage

Another parameter that could affect the biosorption capacity is the biosorbent dosage. Thus, the effect of biosorbent dosage range between 1.0-5.0 g.L^{-1} on the CV removal from aqueous solution was examined at the optimum pH of 7.5 for 100 ppm dye concentration. The equilibrium uptake capacity (q_e; *mg.g*$^{-1}$) and the removal efficiency values of the biosorbent at various biosorbent dosage was calculated and presented in Figure 4. It was realized that the biosorbent concentration frankly shifted the removal efficiency from *ca.*85.6 % to *ca.*92.0% by increasing the mass fraction of the biosorbent. This increment was mainly caused by the increasing the number of active sites. On the other hand, due to the economical and practical reasons 3.0 g.L^{-1} biosorbent dosage was determined as the optimum biosorbent dosage since it was realized that there was no remarkable difference in removal % of 3.0 g.L^{-1} and 5.0 g.L^{-1} biosorbent concentration. Hence, the further experiments were conducted at pH 7.5, and 3.0 g.L^{-1} biosorbent dosage.

3.2.3. Initial Dye Concentration

The dye removal efficiency and the adsorption rate was investigated for various initial CV concentration ranging between 25.0 ppm and 750 ppm at the optimum pH of 7.5 for 120 min at 25 ℃ . The biosorption of CV onto GCs was increased remarkably by increasing the initial dye concentration since the concentration difference offers a significant driving force that could eliminate the mass transfer resistance (Figure 5a.). Figure 5a indicated that the biosorption process significantly depends on the initial dye concentration and *ca.*15 min of contact time is sufficient for reaching the biosorption equilibrium. Within the first 10 min of the biosorption process, it was determined that the major part of the dye species successfully transferred from the dye solution to the solid-liquid interface and adsorb onto the biosorbent active sites. Subsequently, by reaching the equilibrium the biosorption uptake capacity curve reached a plateu (Figure 5a). Moreover, as a result of increasing the number of interactions between the biosorbent and dye species at higher dye concentrations, the biosorption rate was substantially increased up to 4.5 mg.g^{-1}.min^{-1} at 750 ppm initial CV concentration (Figure 5b). On the other hand, it was realized that the removal efficiency of GCs was not boosted by the increase of initial dye concentration since the number of available vacant active sites on the surface of the biosorbent was diminished at the higher dye concentrations.

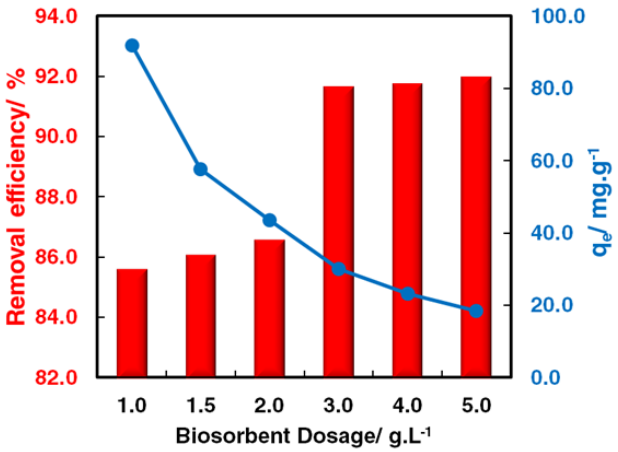

Figure 4. Effects of GCs dosage (g.L^{-1}) on uptake of CV (initial pH=7.5, C_o=100 ppm, t=120 min, T= 25 ℃)

3.2.4. Temperature

The operating temperature of the biosorption process is one of the critical parameters that affects the biosorption rate and the removal efficiency of the biosorbent. The biosorption rate, removal efficiency, and equilibrium dye uptake capacity of the GCs were evaluated at different operating temperatures of 25 ℃, 35 ℃, and 45 ℃ at optimum initial solution pH of 7.5, and 3.0 g.L^{-1} biosorbent dosage. The temperature-dependent biosorption behavior of the GCs indicated its exothermic character since the removal efficiency and biosorption rate values were decreased with the increase of the operating temperature. The equilibrium uptake capacity (q_{eq}) of the GCs decreased from 30.5 mg.g^{-1} to 23.9 mg.g^{-1} by increasing the temperature from 25 to 45 ℃, at pH 7.5 and 100 ppm initial CV concentration. This behavior was attributed to the weakened physical bounding at higher temperatures.

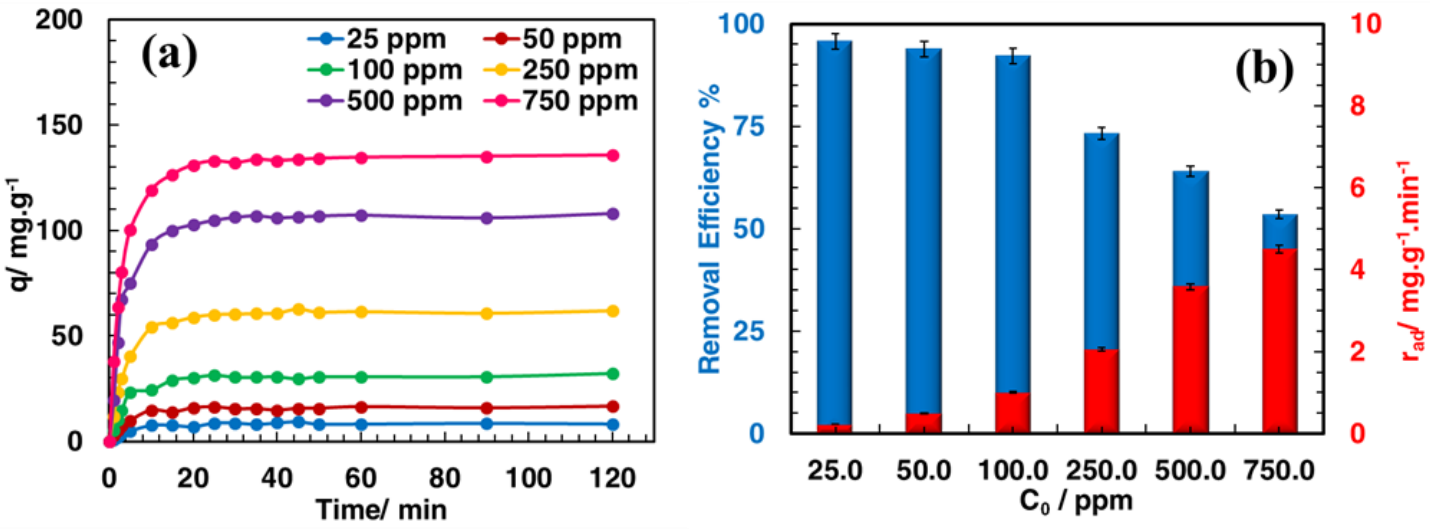

Figure 5. (a)Effect of contact time (b) initial CV concentration on uptake of CV (initial pH=7.5, X=3.0 g.L^{-1}, T= 25 ℃)

Table 3. Effect of operating temperature and initial dye concentration on bisorption rate (r_{ad}), equilibrium uptake capacity (q_{eq}), and CV removal % (initial pH=7.5, X: 3.0 g.L^{-1}).

T	*C_0 (ppm)*	*r_{ad} (mg.g^{-1}.min^{-1})*	*q_{eq} (mg.g^{-1})*	*Removal %*
25	25	0.23	8.2	98.4
	50	0.50	15.0	90.0
	100	1.02	30.5	91.5
	250	2.05	61.5	73.8
	500	3.58	107.4	64.4
	750	4.50	135.0	54.0
35	25	0.23	7.0	81.3
	50	0.44	13.2	75.6
	100	0.87	26.1	77.0
	250	1.72	51.7	61.2
	500	2.96	88.9	53.2
	750	3.72	111.6	44.5
45	25	0.19	5.6	66.9
	50	0.35	10.5	61.9
	100	0.80	23.9	71.1
	250	1.62	48.6	58.3
	500	2.49	74.7	44.7
	750	3.20	95.9	38.3

3.3. Optimal Artificial Neural Network

An optimal ANN was developed with four independent input variables including initial pH of the solution, biosorbent dosage, initial dye concentration, and operating temperature by using MatLab® software. The database was consisted of 200 experimental input and output pairs. Various hidden layer topologies were evaluated to optimize the ANN performance, and the performance metrics were listed in Table 4. The best network performance parameters were obtained for two hidden layers with 5 and 10 neurons in each layer. It was observed that the performance of the network increased with the increasing of the number of hidden layers. The results revealed that the performance of the ANN model was deped on the number of hidden layers and the neurons. The minimum *MSE* and the maximum *R* values of testing data were calculated to be 0.0004 and 0.9995 for hidden layer topology configuration #4. Therefore, as illustrated in Figure 6., the ANN architecture 4-5-10-1, trained by the Levenberg-Marquardt backpropogation algorithm, was selected as the optimal network to forecast the CV removal efficiency of GCs.

Table 4. ANN performance for different hidden layer topologies.

Topology ID	Number of Neurons	Training		Testing	
		MSE	R	MSE	R
#1	[5]	0.0029	0.9959	0.0032	0.9944
2	[10]	0.0009	0.9996	0.0012	0.9992
#3	[5 5]	0.0010	0.9992	0.0015	0.9987
#4	***[5 10]***	***0.0003***	***0.9997***	***0.0004***	***0.9995***
#5	[10 5]	0.0003	0.9997	0.0007	0.9993
#6	[5 5 5]	0.0008	0.9996	0.0011	0.9994
#7	[5 5 5 5]	0.0010	0.9994	0.0010	0.9992

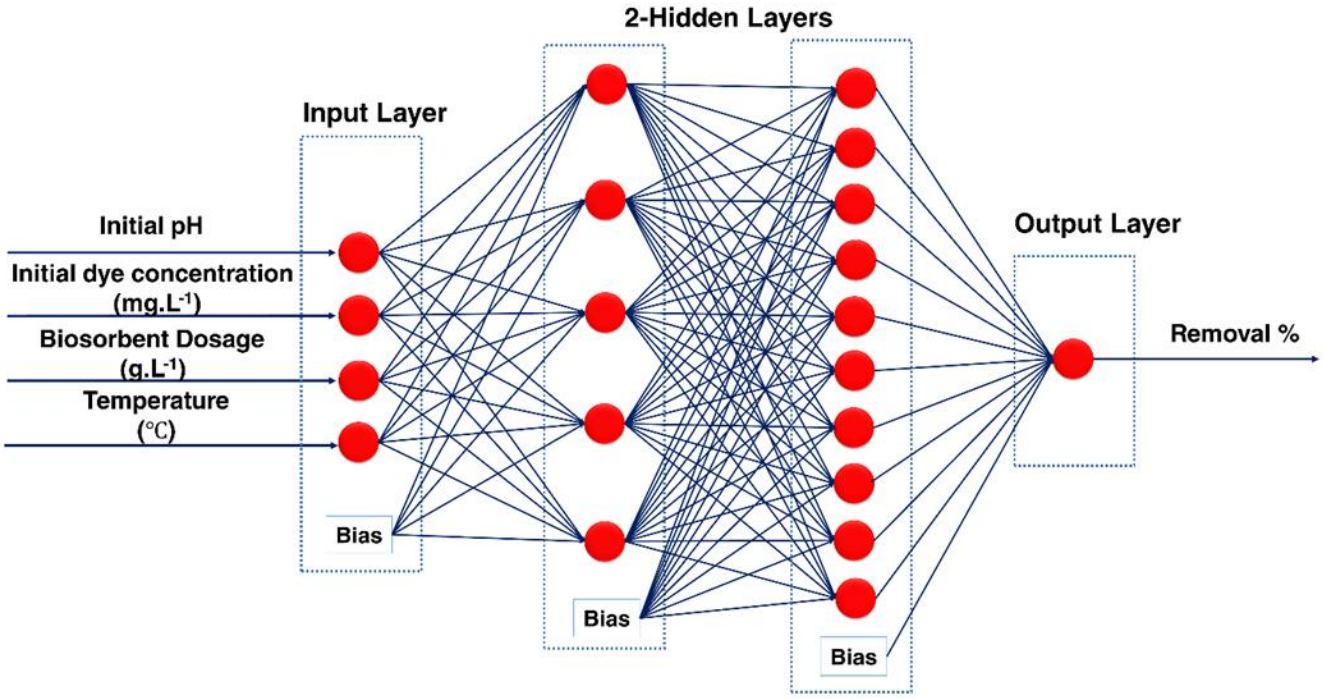

Figure 6. Structure of optimal artificial neural network model

The ANN-predicted and experimental biosorption behaviors of GCs at different operating temperatures and various initial dye concentrations were depicted in Figure 7. The graphs corroborated with the applicability of the proposed optimal ANN in forecasting the CV biosorption onto the GCs since the experimental data and ANN-predicted data were in good agreement.

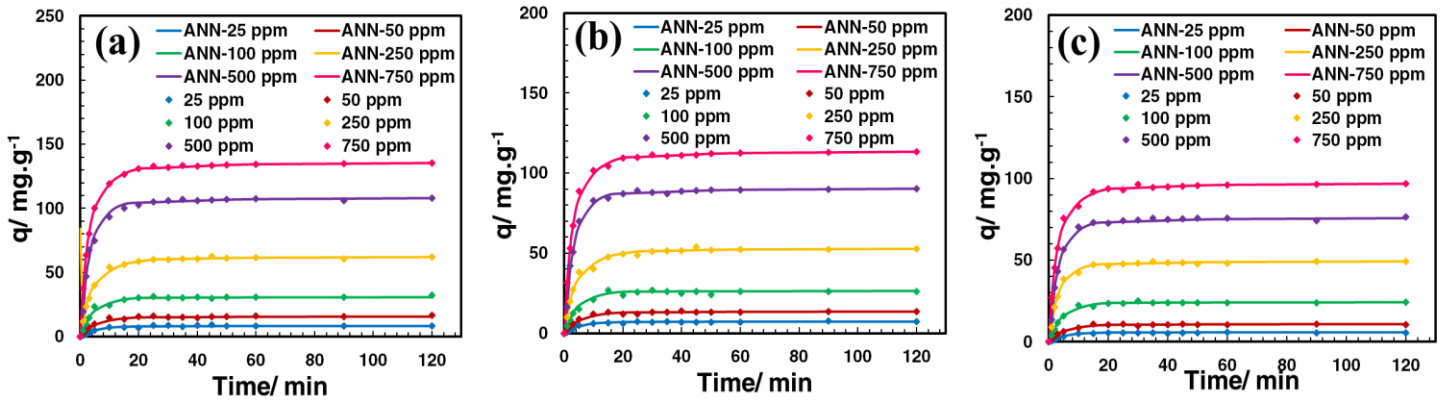

Figure 7. Experimental and ANN-predicted biosorption of CV on GC at different temperatures of (a)25 ℃ (b)25 ℃ (c) 45 ℃ (initial pH=7.5, X=3.0 g.L^{-1})

Figure 8. exhibited the plot of the normalized experimental and ANN-predicted output variable for CV biosorption onto GC during the training and test stages for each input variable. The satisfying harmony between the experimental and the ANN-predicted data demonstrated the good generalization feature of the optimized ANN-model.

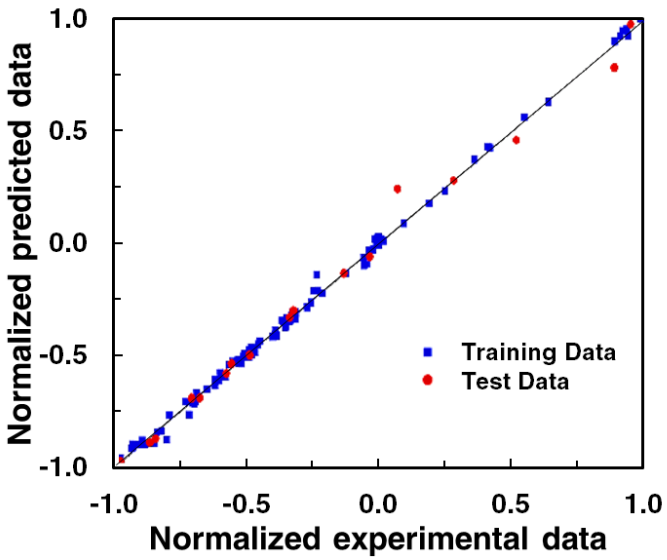

Figure 8. Comparison of the normalized experimental data with ANN-predicted data (initial pH=7.5, C_o=100 ppm, X=3.0 g.L^{-1}, T= 25 ℃)

4. Conclusions and Recommendations

This work proposed a rational route for converting agricultural waste to a value-added material to be utilized in textile wastewater treatment and developed an optimized ANN model for forecasting cationic dye removal from aqueous media. With this scope, the waste orange peel was used as a carbon precursor to produce a carbonaceous biosorbent. As a result, GC with high specific surface area and ordered micro/mesoporous structure were synthesized via an environmentally friendly two step low-cost production pathway. The effect of initial pH of the solution, initial dye concentration, the biosorbent dosage, and the operating temperature of the biosorption process on the biosorption capacity and the removal efficiency of the GC were investigated. The optimum biosorption conditions of CV onto GCs were experimentally determined to be pH 7.5, 3.0 g.L^{-1} biosorbent dosage, and 25 ℃ operating temperature. At the optimal conditions, the experimental results proved that almost 92% of CV could be successfully removed from aqueous solution by utilizing GCs as biosorbent. Furthermore, the ANN approach was applied to forecast the removal efficiency of the biosorbent. Four different independent variables including initial pH of the solution, initial dye concentration, the biosorbent dosage, and the operating temperature were used as input parameters to train the ANN model. The developed ANN model was trained by the Levengberg-Marquardt backpropagation algorithm. The various hidden layer topologies were tested to optimized-ANN model, and the optimal ANN model was established as 4-5-10-1 with R= 0.9995 and MSE=0.0004. The simulations confirmed the proposed ANN model was able to forecast the entire experimental dataset with higher performance metrics. Thus, it can be speculated that GC can be applied as a low-cost alternative biosorbent for removal of cationic dyes from aqueous media and the developed ANN model stands out as a high-performance technique to forecast the CV biosorption onto GC.

References

Abid, M., Niazi, N. K., Bibi, I., Farooqi, A., Ok, Y. S., Kunhikrishnan, A., ... & Arshad, M. (2016). Arsenic (V) biosorption by charred orange peel in aqueous environments. *International journal of phytoremediation*, *18*(5), 442-449.

Broujeni, B. R., Nilchi, A., Azadi, F. (2021). Adsorption modeling and optimization of thorium (IV) ion from aqueous solution using chitosan/TiO2 nanocomposite: Application of artificial neural network and genetic algorithm. *Environmental Nanotechnology, Monitoring & Management*, *15*, 100400.

Das, S. K., Das, A. R., & Guha, A. K. (2007). A study on the adsorption mechanism of mercury on Aspergillus versicolor biomass. *Environmental science & technology*, *41*(24), 8281-8287.

Dehghani, M. H., Yetilmezsoy, K., Salari, M., Heidarinejad, Z., Yousefi, M., & Sillanpää, M. (2020). Adsorptive removal of cobalt (II) from aqueous solutions using multi-walled carbon nanotubes and γ-alumina as novel adsorbents: Modelling and optimization based on response surface methodology and artificial neural network. *Journal of Molecular Liquids*, *299*, 112154.

Elemen, S., Kumbasar, E. P. A., & Yapar, S. (2012). Modeling the adsorption of textile dye on organoclay using an artificial neural network. *Dyes and Pigments*, *95*(1), 102-111.

Fawzy, M., Nasr, M., Nagy, H., & Helmi, S. (2018). Artificial intelligence and regression analysis for Cd (II) ion biosorption from aqueous solution by Gossypium barbadense waste. *Environmental Science and Pollution Research*, *25*(6), 5875-5888.

Ghaedi, M., Ghaedi, A. M., Abdi, F., Roosta, M., Sahraei, R., & Daneshfar, A. (2014). Principal component analysis-artificial neural network and genetic algorithm optimization for removal of reactive orange 12 by copper sulfide nanoparticles-activated carbon. *Journal of Industrial and Engineering Chemistry*, *20*(3), 787-795.

El Hanandeh, A., Mahdi, Z., & Imtiaz, M. S. (2021). Modelling of the adsorption of Pb, Cu and Ni ions from single and multi-component aqueous solutions by date seed derived biochar: Comparison of six machine learning approaches. *Environmental Research*, *192*, 110338.

Karaman, C., Aktas, Z., Bayram, E., Karaman, O., & Kızıl, Ç. (2020). Correlation Between the Molecular Structure of Reducing Agent and pH of Graphene Oxide Dispersion On the Formation of 3D-Graphene Networks. *ECS Journal of Solid State Science and Technology*, *9*(7), 071003.

Karaman, C., Aksu, Z. (2020). Modelling of Remazol Black-B adsorption on chemically modified waste orange peel: pH shifting effect of acidic treatment. *Sakarya University Journal of Science*, *24*(5), 1127-1142.

Karaman, C. (2020). Modeling of Biosorption of Arsenic (V) On Waste Orange Peel Derived Graphene-Like Porous Carbon by Artificial Neural Network Approach. *European Journal of Science and Technology*, 91-100.

Kodal, Süheyla Pınar, and Zümriye Aksu. "Cationic surfactant-modified biosorption of anionic dyes by dried Rhizopus arrhizus." *Environmental technology* 38, no. 20 (2017): 2551-2561.

Liang, S., Guo, X., Feng, N., & Tian, Q. (2009). Application of orange peel xanthate for the adsorption of Pb^{2+} from aqueous solutions. *Journal of Hazardous Materials*, *170*(1), 425-429.

Lu, D., Cao, Q., Li, X., Cao, X., Luo, F., & Shao, W. (2009). Kinetics and equilibrium of Cu (II) adsorption onto chemically modified orange peel cellulose biosorbents. *Hydrometallurgy*, *95*(1-2), 145-152.

Pathak, P. D., Mandavgane, S. A., & Kulkarni, B. D. (2016). Characterizing fruit and vegetable peels as bioadsorbents. Current Science, 2114-2123.

Pauletto, P. S., Dotto, G. L., & Salau, N. P. (2020). Optimal artificial neural network design for simultaneous modeling of multicomponent adsorption. *Journal of Molecular Liquids*, *320*, 114418.

Rahaman, M. S., Basu, A., & Islam, M. R. (2008). The removal of As (III) and As (V) from aqueous solutions by waste materials. Bioresource technology, 99(8), 2815-2823.

Su, T., Guan, X., Tang, Y., Gu, G., & Wang, J. (2010). Predicting competitive adsorption behavior of major toxic anionic elements onto activated alumina: A speciation-based approach. *Journal of hazardous materials*, *176*(1-3), 466-472.